ChemistryOpen

Research Article
doi.org/10.1002/open.202100254

Chemistry Europe
European Chemical Societies Publishing

www.chemistryopen.org

Insights into the Activation Mode of α-Carbonyl Sulfoxonium Ylides in Rhodium-Catalyzed C–H Activation: A Theoretical Study

Dianmin Zhang,[a] Xiaofang He,[a] Tao Yang,[a] and Song Liu*[a, b]

A computational study has been performed to investigate the mechanism of Rh^{III}-catalyzed C–H bond activation using sulfoxonium ylides as a carbene precursor. The stepwise and concerted activation modes for sulfoxonium ylides were investigated. Detailed theoretical results showed that the favored stepwise pathway involves C–H bond activation, carbonization, carbene insertion, and protonation. The free energy profiles for dialkylation of 2-phenylpyridine were also calculated to account for the low yield of this reaction. Furthermore, the substituent effect was elucidated by comparing the energy barriers for the protonation of *meta*- and *para*-substituted sulfoxonium ylides calculated by density functional theory.

Introduction

Construction of C–C bonds is a major area of both academic and industrial chemistry. The ubiquity and low cost of hydrocarbons make C–H bond functionalization an attractive alternative to classical transition-metal-catalyzed cross-coupling reactions with functionalized organic compounds.[1] In recent years, transition-metal-catalyzed C–H bond activation has developed into an efficient, atom- and step-economical strategy for C–C bond construction.[2] In particular, metal-carbene insertion into $C(sp^2)$–H bonds has emerged as a common approach for constructing $C(sp^2)$–$C(sp^3)$ bonds.[3] This strategy is mainly considered to follow a pathway comprising $C(sp^2)$–H metalation, metal carbene formation, carbene migratory insertion, and protonation (Scheme 1).[4]

In recent years, Cp^*Rh^{III} ($Cp^* = 1,2,3,4,5$-pentamethylcyclopentadienyl) complexes have shown significant catalytic activity in C–H functionalization.[5] A wide range of carbene precursors, including α-diazo carbonyls, hydrazones, triazo compounds, cyclopropenes, and ketone-functionalized enynes, have been explored as coupling partners in Cp^*Rh^{III}-catalyzed direct aryl C–H activation to construct $C(sp^2)$–$C(sp^3)$ bonds. Direct dediazoniation of α-diazo carbonyls in the presence of Cp^*Rh^{III} generates Cp^*Rh^{III}–Carbene complexes (Scheme 2a).[6] The Cp^*Rh^{III}–Carbene complex results from dediazoniation of the diazo substrate generated in situ from a hydrazone in the presence of a base (Scheme 2b).[7] Additionally, 1,2,3-triazoles share the characteristics of diazo compounds because of the equilibrium between the closed and open forms (Scheme 2c).[8] Cyclopropenes can also be used as vinyl Cp^*Rh^{III}–Carbene precursors through ring opening (Scheme 2d).[9] The Lewis-acidic Rh^{III} center can readily initiate a 5-exo-dig cyclization in ketone-functionalized enynes to afford Cp^*Rh^{III}–Carbene complexes (Scheme 2e).[10] Furthermore, coordination of iodonium ylide and subsequent elimination of PhI can also give Cp^*Rh^{III}–Carbene (Scheme 2f).[11]

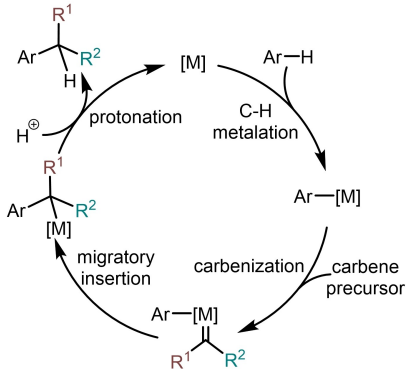

Scheme 1. C–H bond functionalization with metal carbenes.

In 2017, Aïssa[12] and Li[13] independently reported Cp^*Rh^{III}-catalyzed arene C–H bond activation and acylmethylation using sulfoxonium ylides[14] as a carbene precursor. The products were isolated in good to high yields from a range of 2-sulfoxonium ylides bearing aryl, heteroaryl, cyclopropyl, and adamantyl ketone groups (Scheme 3). The previously reported plausible catalytic cycle, based on experimental observations, features

[a] D. Zhang, X. He, T. Yang, Dr. S. Liu
Chongqing Key Laboratory of Environmental Materials and Remediation Technologies
College of Chemistry and Environmental Engineering,
Chongqing University of Arts and Sciences
Chongqing, 402160 (China)
E-mail: sliu@cqwu.edu.cn
[b] Dr. S. Liu
School of Chemistry and Chemical Engineering
Chongqing University
Chongqing 400030 (China)

Supporting information for this article is available on the WWW under https://doi.org/10.1002/open.202100254

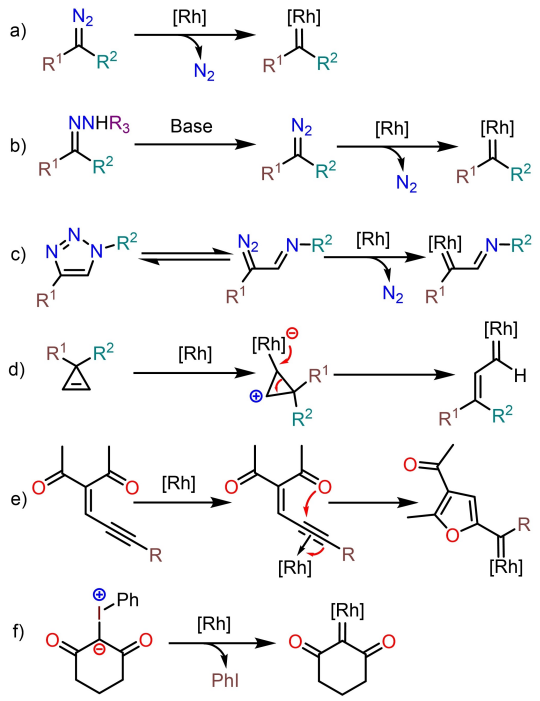

Scheme 2. Activation mode of carbene precursors in Cp*Rh^{III}-catalyzed C–H bond functionalization.

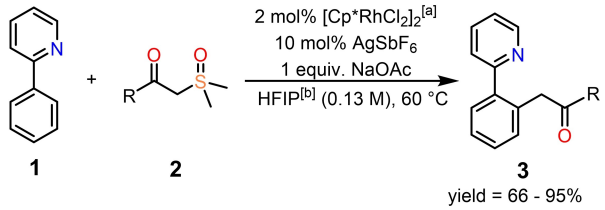

Scheme 3. Cp*Rh^{III}-catalyzed C–H bond activation using a sulfoxonium ylide as a carbene precursor. [a] Cp* = 1,2,3,4,5-pentamethylcyclopentadienyl. [b] HFIP = 1,1,1,3,3,3-hexafluoro-2-propanol.

C–H activation, migratory insertion of the ylide into the carbon–metal bond, and protodemetalation, but the detailed activation mode for the α-carbonyl sulfoxonium ylides remains unclear. Whether migratory insertion of α-carbonyl sulfoxonium ylides into C(aryl)-Rh^{III} bonds occurs through a concerted or stepwise mechanism is disputed.

Herein, we report a computational study of the mechanism of the reaction reported by Aïssa.[12] The detailed reaction mechanism of this Cp*Rh^{III}-catalyzed arene C–H bond acylmethylation reaction using sulfoxonium ylides as a carbene precursor was elucidated. The potential energy surface for dialkylation of the 2-phenylpyridine substrate was also calculated to account for the low yield of the dialkylation product reported by Li.[13] Furthermore, Hammett plots with some representative substituents on α-carbonyl sulfoxonium ylides were applied to study the electronic effect of the rate-determining step.

Computational Methods

All of the density functional theory (DFT) calculations were performed with using the Gaussian 09 series of programs.[15] The B3-LYP[16] density functional with the standard 6-31G(d) basis set (SDD basis set for Rh and I) was used for the geometry optimizations. Harmonic frequency calculations were performed for all of the stationary points to confirm whether they are as local minima or transition structures, and to derive the thermochemical corrections for the enthalpies and free energies. All of the minima had zero imaginary frequency and all of the transition states had only one imaginary frequency. The M06 functional with larger basis set 6-311 + G(d) (SDD basis set for Rh and I) was used to calculate the single point energies with 1,1,1,3,3,3-hexafluoro-2-propanol as the solvent using a continuum solvation model (SMD).[17] For the solvent data not included in Gaussian 09, the key parameters were set in the input file manually (for 1,1,1,3,3,3-hexafluoro-2-propanol, eps = 16.70, while the other parameters were the same as for 2-propanol). The reported energies are the M06-calculated Gibbs free energies in 1,1,1,3,3,3-hexafluoro-2-propanol solvent. The optimized structures were visualized using CYLview.[18]

Results and Discussion

The proposed catalytic cycles for Cp*Rh^{III}-catalyzed C–H bond activation using sulfoxonium ylides as a carbene precursor are shown in Scheme 4. Two possible pathways, with cationic Cp*Rh^{III} complex **A** set as the active catalytic complex, were considered during computational modeling of the reaction. Coordination of the 2-phenylpyridine substrate to cationic Cp*Rh^{III} complex **A** and subsequent electrophilic deprotonation affords five-membered rhodacyclic intermediate **B**. Subsequent coordination of sulfoxonium ylide **2** gives alkyl-Rh^{III} species **C**, which then undergoes β-elimination of dimethyl-sulfoxide (DMSO) to afford reactive carbene-Rh^{III} species **D** (pathway A). Migratory insertion of the activated carbene into the aryl-Rh bond generates alkyl-Rh^{III} species **E**. Finally, acylmethylation

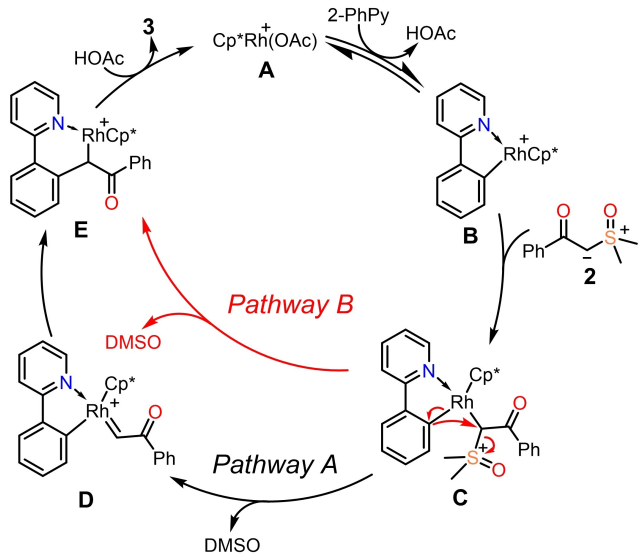

Scheme 4. Proposed catalytic cycle for Cp*Rh^{III}-catalyzed C–H bond activation using a sulfoxonium ylide as a carbene precursor.

product **3** is generated by protonation of intermediate **E** by acetic acid, and the active catalyst, cationic Cp*Rh^{III} complex **A**, is regenerated to complete the catalytic cycle. In pathway B, an S_N2-type displacement of DMSO by the aryl group in intermediate **C** gives alkyl-Rh^{III} species **E**. Both pathways were investigated by DFT calculations.

The calculated Gibbs energy profile for pathway A is shown in Figure 1, in which cationic Cp*Rh^{III} species **CP1** is set as the relative zero point. Coordination of 2-phenylpyridine substrate **1** to the Rh^{III} center gives intermediate **CP2**, which is 5.7 kcal mol^{-1} exergonic. Subsequent pyridyl-directed electrophilic deprotonation occurs via transition state **TS1** with an energy barrier of 17.0 kcal mol^{-1}, from which five-membered rhodacyclic intermediate **CP3** is generated. In transition state **TS1**, the lengths of the breaking C–H and forming O–H bonds are 1.32 and 1.33 Å, respectively, while the length of the forming C–Rh bond is 2.23 Å. The free energy of **CP3** is 5.2 kcal mol^{-1} higher than that of **CP2**. The calculated results indicate that the first C–H bond activation is reversible, which is consistent with the results of H/D exchange experiments. Coordination of sulfoxonium ylide **2** to the Rh^{III} center in **CP3** gives alkyl-Rh^{III} intermediate **CP4**, which is 10.3 kcal mol^{-1} exergonic.

Subsequent β-elimination of DMSO in **CP4** occurs via transition state **TS2** to afford reactive carbene-Rh^{III} intermediate **CP5**. The structural information regarding **TS2** shows that the length of the breaking C–S bond is 2.45 Å. Migratory insertion of the carbene into the aryl-Rh bond generates six-membered alkyl-Rh^{III} species **CP6** via transition state **TS3** with an energy barrier of only 3.6 kcal mol^{-1}. The structural information of **TS3** shows that the lengths of the forming C–C and the breaking C–Rh bonds are 2.39 and 2.10 Å, respectively. Coordination of acetic acid to the Rh^{III} center in **CP6** gives **CP7**, which is 6.3 kcal mol^{-1} endergonic. Subsequent protonation of the alkyl-Rh^{III} bond by acetic acid occurs via transition state **TS4** with an overall activation free energy of 28.4 kcal mol^{-1} to give **CP8**. In **TS4**, the lengths of the forming C–H and breaking O–H bonds are 1.43 and 1.26 Å, respectively. The calculated results show that the protonation process is the rate-determining step in the Cp*Rh^{III}-catalyzed C–H bond acylmethylation reaction, which is consistent with experimental observations. Final ligand exchange of 2-phenylpyridine substrate **1** with acylmethylation

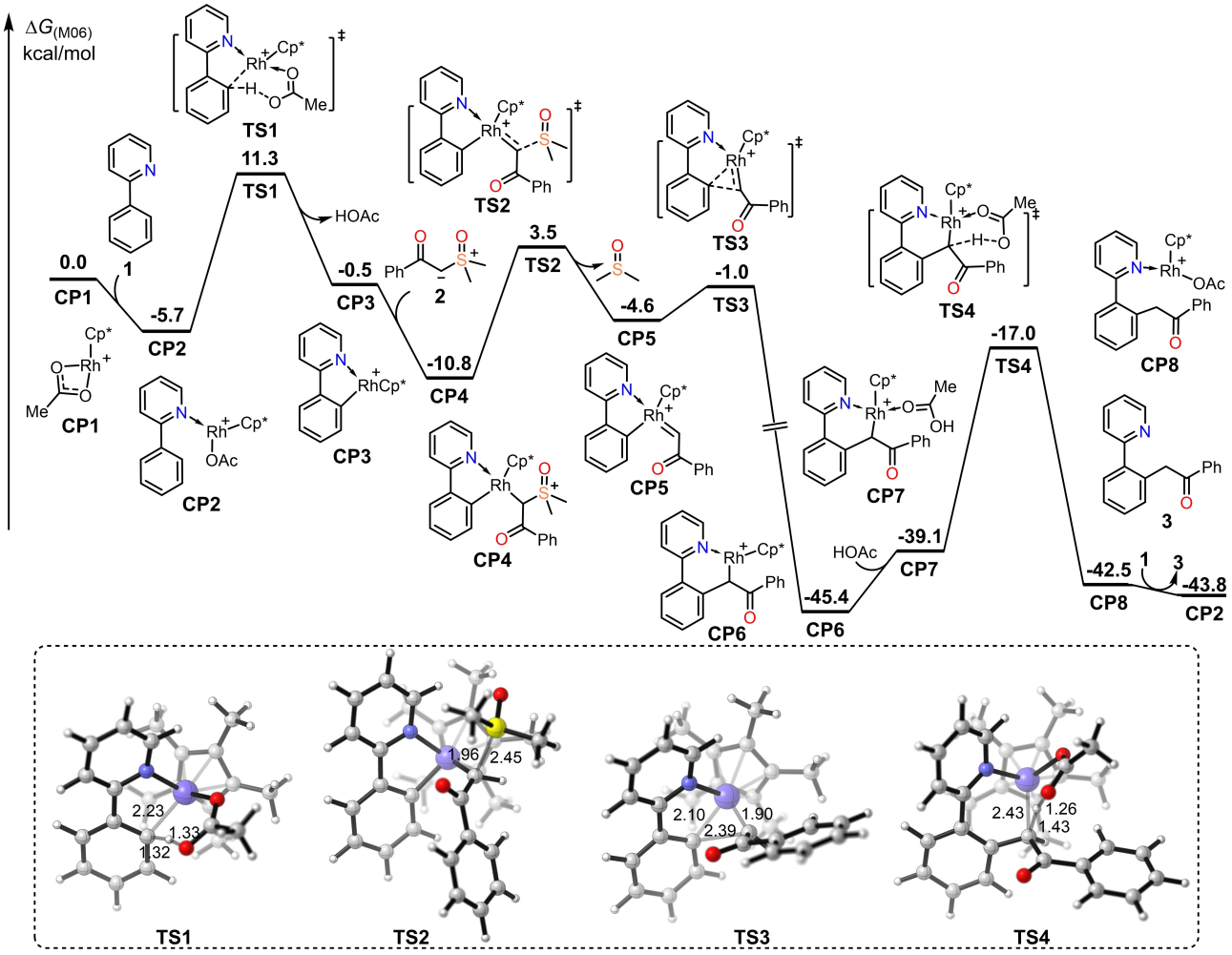

Figure 1. Gibbs energy profile and structural information for pathway A of Cp*Rh^{III}-catalyzed C–H bond activation using a sulfoxonium ylide as a carbene precursor. Values for bond lengths are given in angstroms (Å).

product **3** gives active catalytic intermediate **CP2**, completing the catalytic cycle.

The calculated free energy profiles of the S_N2-type displacement pathway are shown in Figures 2 and 3. As shown in Figure 2, coordination of the carbonyl group in sulfoxonium ylides **2** to the Rh^{III} center in **CP3** gives intermediate **CP9**, which is 6.2 kcal mol^{-1} exergonic. Subsequent S_N2-type displacement of DMSO by the aryl group in intermediate **CP9** occurs via concerted transition state **TS5** to generate enol-Rh^{III} species **CP10**.The energy barrier for this step is 51.5 kcal mol^{-1}, which indicates that this pathway is unfavorable. The geometric information of **TS5** shows that the lengths of the forming C–H and breaking C–S bonds are 1.67 and 1.88 Å, respectively, while the length of the breaking C–Rh bond is 2.25 Å. The structural information of **TS5** indicates a concerted process.

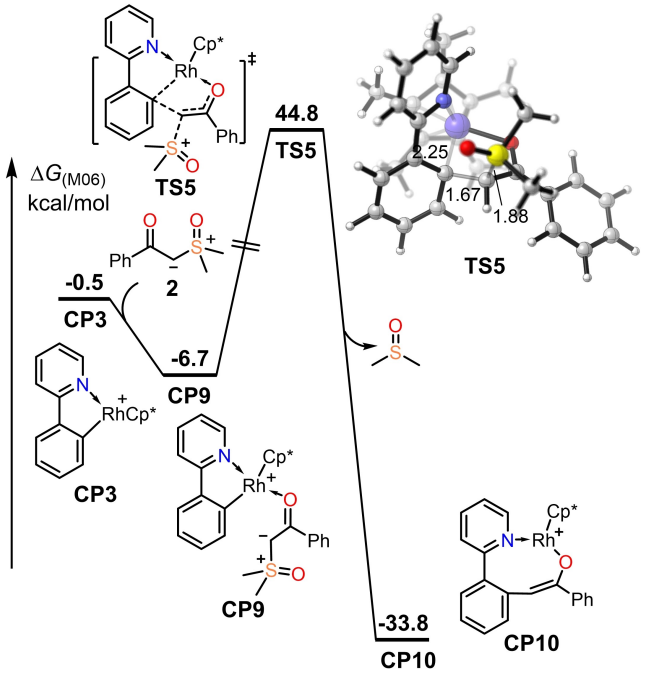

Figure 2. Gibbs energy profile and structural information for pathway B of Cp*Rh^{III}-catalyzed C–H bond activation using a sulfoxonium ylide as a carbene precursor. Values for bond lengths are given in angstroms (Å).

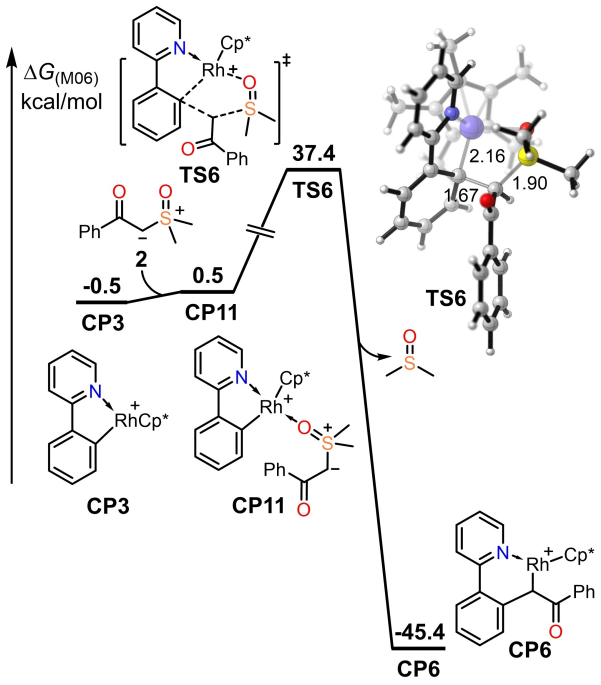

Figure 3. Gibbs energy profile and structural information for pathway B of Cp*Rh^{III}-catalyzed C–H bond activation using a sulfoxonium ylide as a carbene precursor. Values for bond lengths are given in angstroms (Å).

As shown in Figure 3, the coordination of sulfoxonium ylide **2** to the Rh^{III} center by the sulfoxide group gives complex **CP11**, which is 1.0 kcal mol^{-1} endergonic. The subsequent concerted S_N2-type displacement process occurs via transition state **TS6** with an energy barrier of 37.9 kcal mol^{-1} to generate **CP6**. The free energy of **TS6** is 33.9 kcal mol^{-1} higher than that of **TS2**, which indicates that this concerted S_N2-type displacement pathway is also unfavorable.

In Li's work,[13] when 2-phenylpyridine was used as the substrate, $Zn(OAc)_2$ as additive, both mono- and dialkylation products were obtained in a 2:1 ratio (Scheme 5). DFT calculations are performed to account for this observation. The calculated potential energy surface for dialkylation of the 2-phenylpyridine substrate is shown in Figure S1 (see the Supporting Information for details). Pyridyl-directed electrophilic deprotonation of **CP8** occurs via transition state **TS7** with an energy barrier of 21.3 kcal mol^{-1} to give five-membered rhodacyclic intermediate **CP12**. The free energy of **TS7** is 5.6 kcal mol^{-1} higher than that of **TS1**, which results in the low yield of the dialkylation product.

Hammett plots[19] with some representative substituents (NH_2, CH_3, OMe, F, Cl, Br, I, CN, and NO_2) were then applied to study the electronic effect of the rate-determining step in the Cp*Rh^{III}-catalyzed C–H bond acylmethylation reaction. As shown in Figure 4, for both the *meta*- and *para*-positions of the aryl ketones in the sulfoxonium ylide, a negative Hammett effect was found. The calculated results indicate that an electron-donating substituent on the aryl ketone in sulfoxonium ylides would increase the ionic character of the C(alkyl)-Rh^{III} bond, leading to a lower protonation barrier, which is consistent with the experimental results showing that electron-donating substituents are favorable in terms of the reaction yield. The slope of the calculated Hammett plot for *meta*-position substitution of the aryl ketone in sulfoxonium ylides was 0.15, while that for the *para* position was 0.09. The greater conjugate effect of *meta*-position substitution than *para*-position substitution on the ionic character of the C–Rh bond in the protonation transition state leads to the lower slope. Furthermore, *meta*-position substitution showed a better correlation than *para*-position substitution.

Conclusion

In summary, the M06 DFT method has been used to examine the mechanism of Cp*Rh^{III}-catalyzed C–H bond activation using sulfoxonium ylide as a carbene precursor. The theoretical

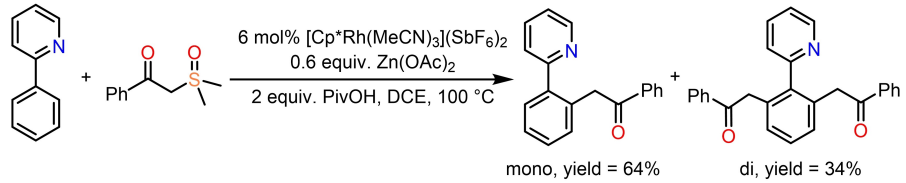

Scheme 5. Rh^{III}-catalyzed C–H mono- and dialkylation of arenes using a sulfoxonium ylide as a carbene precursor.

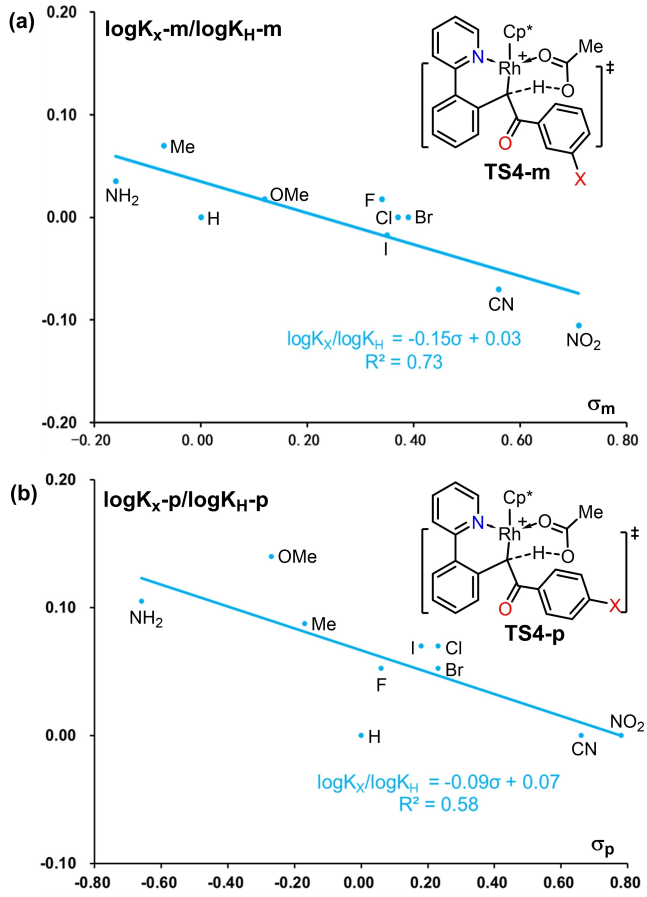

Figure 4. Hammett plots for the (a) *meta*-position and (b) *para*-position in the protonation process.

calculations indicated that this reaction proceeds through C–H bond activation, carbonization, carbene insertion, and protonation. The rate-determining step was found to be protonation, which is consistent with the experimental results. The calculated results showed that activation of the sulfoxonium ylide occurs through a stepwise pathway rather than a concerted pathway. The high activation energy of the second C–H bond activation leads to the low experimental yield of the dialkylation product. Furthermore, Hammett plot calculations indicated that the rate-determining protonation step was more efficient if an electron-donating substituent was present on the aryl ketone in the sulfoxonium ylide. In addition, *meta*-position substitution of the aryl ketone had a greater effect on the rate of the protonation step than *para*-position substitution.

Acknowledgements

This project was supported by the Basic and Frontier Research Project of Chongqing Science and Technology Commission (no. cstc2021jcyj-msxmX0593) and the Scientific Research Fund of Chongqing University of Arts and Sciences (nos. R2020SHH01 and P2021HH03). This project was also funded by the Project of Scientific and Technological Research Program of Chongqing Municipal Education Commission (no. KJQN202101301).

Conflict of Interest

The authors declare no conflict of interest.

Data Availability Statement

The data that support the findings of this study are available in the supplementary material of this article.

Keywords: carbene · Cp*Rh^{III}-catalyzed · C–H bond activation · reaction mechanisms · theoretical study

[1] a) G. Dyker, *Angew. Chem. Int. Ed.* **1999**, *38*, 1698–1712; *Angew. Chem.* **1999**, *111*, 1808–1822; b) F. Kakiuchi, S. Murai, *Acc. Chem. Res.* **2002**, *35*, 826–834; c) I. V. Seregin, V. Gevorgyan, *Chem. Soc. Rev.* **2007**, *36*, 1173–1193; d) R. Giri, B. F. Shi, K. M. Engle, N. Maugel, J. Q. Yu, *Chem. Soc. Rev.* **2009**, *38*, 3242–3272; e) J. Wencel-Delord, T. Droge, F. Liu, F. Glorius, *Chem. Soc. Rev.* **2011**, *40*, 4740–4761; f) Y. Park, Y. Kim, S. Chang, *Chem. Rev.* **2017**, *117*, 9247–9301; g) J. R. Hummel, J. A. Boerth, J. A. Ellman, *Chem. Rev.* **2017**, *117*, 9163–9227; h) C.-S. Wang, P. H. Dixneuf, J.-F. Soulé, *Chem. Rev.* **2018**, *118*, 7532–7585; i) Y. Lan, *Computational Methods in Organometallic Catalysis*. Wiley-VCH; Weinheim: **2021**; j) J. Zhang, X. Lu, C. Shen, L. Xu, L. Ding, G. Zhong, *Chem. Soc. Rev.* **2021**, *50*, 3263–3314.

[2] a) V. Ritleng, C. Sirlin, M. Pfeffer, *Chem. Rev.* **2002**, *102*, 1731–1770; b) X. Chen, K. M. Engle, D.-H. Wang, J.-Q. Yu, *Angew. Chem. Int. Ed.* **2009**, *48*, 5094–5115; *Angew. Chem.* **2009**, *121*, 5196–5217; c) E. Nakamura, N. Yoshikai, *J. Org. Chem.* **2010**, *75*, 6061–6067; d) C. S. Yeung, V. M. Dong, *Chem. Rev.* **2011**, *111*, 1215–1292; e) M. Zhang, Y. Zhang, X. Jie, H. Zhao, G. Li, W. Su, *Org. Chem. Front.* **2014**, *1*, 843–895; f) C. Liu, J. Yuan, M. Gao, S. Tang, W. Li, R. Shi, A. Lei, *Chem. Rev.* **2015**, *115*, 12138–12204; g) L. Ping, D. S. Chung, J. Bouffard, S. G. Lee, *Chem. Soc. Rev.* **2017**, *46*, 4299–4328; h) T. Higashi, S. Kusumoto, K. Nozaki, *Chem. Rev.* **2019**, *119*, 10393–10402.

[3] a) M. P. Doyle, *Chem. Rev.* **1986**, *86*, 919–939; b) M. P. Doyle, D. C. Forbes, *Chem. Rev.* **1998**, *98*, 911–936; c) A. J. Arduengo, *Acc. Chem. Res.* **1999**, *32*, 913–921; d) P. de Frémont, N. Marion, S. P. Nolan, *Coord. Chem. Rev.* **2009**, *253*, 862–892; e) M. P. Doyle, R. Duffy, M. Ratnikov, L. Zhou, *Chem. Rev.* **2010**, *110*, 704–724; f) H. M. L. Davies, J. R. Manning, *Nature* **2008**, *451*, 417–424; g) Y. Xia, D. Qiu, J. Wang, *Chem. Rev.* **2017**,

117, 13810–13889; h) D. Zhu, L. Chen, H. Fan, Q. Yao, S. Zhu, *Chem. Soc. Rev.* **2020**, *49*, 908–950; i) S.-J. Li, X. Li, H. Mo, L.-B. Qu, D. Wei, Y. Lan, *Chem. Commun.* **2020**, *56*, 4732–4735; j) T. Wang, A. S. K. Hashmi, *Chem. Rev.* **2021**, *121*, 8948–8978; k) L.-W. Ye, X.-Q. Zhu, R. L. Sahani, Y. Xu, P.-C. Qian, R.-S. Liu, *Chem. Rev.* **2021**, *121*, 9039–9112.

[4] a) Z. Liu, J. Wang, *J. Org. Chem.* **2013**, *78*, 10024–10030; b) F. Hu, Y. Xia, F. Ye, Z. Liu, C. Ma, Y. Zhang, J. Wang, *Angew. Chem. Int. Ed.* **2014**, *53*, 1364–1367; *Angew. Chem.* **2014**, *126*, 1388–1391; c) X. Qi, Y. Lan, *Acc. Chem. Res.* **2021**, *54*, 2905–2915.

[5] a) T. Satoh, M. Miura, *Chem. Eur. J.* **2010**, *16*, 11212–11222; b) D. A. Colby, A. S. Tsai, R. G. Bergman, J. A. Ellman, *Acc. Chem. Res.* **2012**, *45*, 814–825; c) N. Kuhl, N. Schroder, F. Glorius, *Adv. Synth. Catal.* **2014**, *356*, 1443–1460; d) G. Song, X. Li, *Acc. Chem. Res.* **2015**, *48*, 1007–1020; e) B. Ye, N. Cramer, *Acc. Chem. Res.* **2015**, *48*, 1308–1318; f) K. Shin, H. Kim, S. Chang, *Acc. Chem. Res.* **2015**, *48*, 1040–1052; g) S. Yu, S. Liu, Y. Lan, B. Wan, X. Li, *J. Am. Chem. Soc.* **2015**, *137*, 1623–1631; h) T. Gensch, M. N. Hopkinson, F. Glorius, J. Wencel-Delord, *Chem. Soc. Rev.* **2016**, *45*, 2900–2936; i) Y. Li, H. Chen, Li.-B. Qu, K. N. Houk, Y. Lan, *ACS Catal.* **2019**, *9*, 7154–7165; j) F. Wang, J. Jing, Y. Zhao, X. Zhu, X.-P. Zhang, L. Zhao, P. Hu, W.-Q. Deng, X. Li, *Angew. Chem. Int. Ed.* **2021**, *60*, 16628–16633; *Angew. Chem.* **2021**, *133*, 16764–16769; k) F. Wang, Z. Qi, Y. Zhao, S. Zhai, G. Zheng, R. Mi, Z. Huang, X. Zhu, X. He, X. Li, *Angew. Chem. Int. Ed.* **2020**, *59*, 13288–13294; *Angew. Chem.* **2021**, *132*, 13390–13396; l) S. R. Neufeldt, G. Jimenez Oses, J. R. Huckins, O. R. Thiel, K. N. Houk, *J. Am. Chem. Soc.* **2015**, *137*, 9843–9854; m) X. Qi, Y. Li, R. Bai, Y. Lan, *Acc. Chem. Res.* **2017**, *50*, 2799–2808; n) D. L. Davies, S. A. Macgregor, C. L. McMullin, *Chem. Rev.* **2017**, *117*, 8649–8709; o) S. Liu, X. Qi, L.-B. Qu, R. Bai, Y. Lan, *Catal. Sci. Technol.* **2018**, *8*, 1645–1651.

[6] a) W.-W. Chan, S.-F. Lo, Z. Zhou, W.-Y. Yu, *J. Am. Chem. Soc.* **2012**, *134*, 13565–13568; b) Z. Shi, D. C. Koester, M. Boultadakis-Arapinis, F. Glorius, *J. Am. Chem. Soc.* **2013**, *135*, 12204–12207; c) T. K. Hyster, K. E. Ruhl, T. Rovis, *J. Am. Chem. Soc.* **2013**, *135*, 5364–5367; d) Y. Cheng, C. Bolm, *Angew. Chem. Int. Ed.* **2015**, *54*, 12349–12352; *Angew. Chem.* **2015**, *127*, 12526–12529; e) K. S. Halskov, H. S. Roth, J. A. Ellman, *Angew. Chem. Int. Ed.* **2017**, *56*, 9183–9187; *Angew. Chem.* **2017**, *129*, 9311–9315.

[7] a) Y. Xia, J. Wang, *Chem. Soc. Rev.* **2017**, *46*, 2306–2362; b) J. Radolko, P. Ehlers, P. Langer, *Adv. Synth. Catal.* **2021**, *363*, 3616–3654.

[8] a) J. H. Kim, T. Gensch, D. Zhao, L. Stegemann, C. A. Strassert, F. Glorius, *Angew. Chem. Int. Ed.* **2015**, *54*, 10975–10979; *Angew. Chem.* **2015**, *127*, 11126–11130; b) M. Tian, B. Liu, J. Sun, X. Li, *Org. Lett.* **2018**, *20*, 4946–4949.

[9] a) H. Zhang, K. Wang, B. Wang, H. Yi, F. Hu, C. Li, Y. Zhang, J. Wang, *Angew. Chem. Int. Ed.* **2014**, *53*, 13234–13238; *Angew. Chem.* **2014**, *126*, 13450–13454; b) W. Guo, Y. Xia, *J. Org. Chem.* **2015**, *80*, 8113–8121.

[10] S. Y. Hong, J. Jeong, S. Chang, *Angew. Chem. Int. Ed.* **2017**, *56*, 2408–2412; *Angew. Chem.* **2017**, *129*, 2448–2452.

[11] a) Y. Jiang, P. Li, J. Zhao, B. Liu, X. Li, *Org. Lett.* **2020**, *22*, 7475–7479; b) Z. Han, M.-M. Xu, R.-Y. Zhang, X.-P. Xu, S.-J. Ji, *Green Chem.* **2021**, *23*, 6337–6340; c) S. Nunewar, S. Kumar, H. Pandhare, S. Nanduri, V. Kanchupalli, *Org. Lett.* **2021**, *23*, 4233–4238; d) Z. Dong, P. Li, X. Li, B. Liu, *Chin. J. Chem.* **2021**, *39*, 2489–2494.

[12] M. Barday, C. Janot, N. R. Halcovitch, J. Muir, C. Aïssa, *Angew. Chem. Int. Ed.* **2017**, *56*, 13117–13121; *Angew. Chem.* **2017**, *129*, 13297–13301.

[13] Y. Xu, X. Zhou, G. Zheng, X. Li, *Org. Lett.* **2017**, *19*, 5256–5259.

[14] a) J. Vaitla, A. Bayer, K. H. Hopmann, *Angew. Chem. Int. Ed.* **2018**, *57*, 16180–16184; *Angew. Chem.* **2018**, *130*, 16412–16416; b) P. B. Momo, A. N. Leveille, E. H. E. Farrar, M. N. Grayson, A. E. Mattson, A. B. Burtoloso, *Angew. Chem. Int. Ed.* **2020**, *59*, 15554–15559; *Angew. Chem.* **2020**, *132*, 15684–15689; c) C. Lv, X. Meng, M. Wang, Y. Zhang, C. Hu, C. K. Kim, Z. Su, *J. Org. Chem.* **2021**, 86, 11683–11697.

[15] M. J. Frisch et al. Gaussian 09, Revision D.01; Gaussian, Inc.: Wallingford, CT, **2013**.

[16] a) A. D. J. Becke, *Chem. Phys.* **1993**, *98*, 5648–5652; b) C. Lee, W. Yang, R. G. Parr, *Phys. Rev. B* **1988**, *37*, 785–789.

[17] a) M. Cossi, V. Barone, R. Cammi, J. Tomasi, *Chem. Phys. Lett.* **1996**, *255*, 327–335; b) E. Cances, B. Mennucci, J. Tomasi, *J. Chem. Phys.* **1997**, *107*, 3032–3041; c) V. Barone, M. Cossi, J. Tomasi, *J. Comput. Chem.* **1998**, *19*, 404–417; d) A. V. Marenich, C. J. Cramer, D. G. Truhlar, *J. Phys. Chem. B* **2009**, *113*, 6378–6396; e) S.-J. Li, Y. Lan, *Chem. Commun.* **2020**, *56*, 6609–6619.

[18] C. Y. Legault, CYLView, 1.0b; Université de Sherbrooke: Quebec, Canada, **2009**. www.cylview.org (accessed 1/10/2017).

[19] C. Hansch, A. Leo, R. W. Taft, *Chem. Rev.* **1991**, *91*, 165–195.

Manuscript received: November 5, 2021
Revised manuscript received: February 8, 2022